CrossMark

Morphological Observation and Comparative Transcriptomic Analysis of *Clostridium perfringens* Biofilm and Planktonic Cells

Xiaofen Zhang[1,2] · Yuhua Ma[1,2] · Guisheng Ye[1,2]

Abstract

Bacterial biofilms can enhance survival in adverse environments and promote infection. However, little is known about biofilm formation by *Clostridium perfringens*. To better characterize this process, we used SEM to observe the surfaces of *C. perfringens* biofilms after 12, 24, 48, and 72 h of incubation. Biofilm cells appeared to be encased in a dense matrix material, and the total biomass of the biofilm increased with incubation time. To gain insight into the differentially expressed genes (DEGs) between biofilm and planktonic cells, we carried out comparative transcriptomic analysis using RNA sequencing. In total, 91 genes were significantly differentially expressed, with 40 being up-regulated and 51 down-regulated. In particular, genes encoding sortase, ribosomal proteins, and ATP synthase were up-regulated in biofilms, while genes coding for clostripain and phospholipase C were down-regulated. To validate the RNA sequencing results, qRT-PCR analysis was performed using five randomly selected DEGs. Results showed that all five genes were up-regulated, which was in accordance with the RNA sequencing results. To examine the functional differences, the DEGs were characterized by GO and KEGG pathway enrichment analyses. Results showed that the up-regulated genes were divided into 32 significantly enriched GO terms, with "macromolecular complex" being the most common. Oxidative phosphorylation was the only significantly enriched pathway, suggesting that ATP is required for biofilm stability. This study provides valuable insights into the morphology and transcriptional regulation of *C. perfringens* during biofilm formation, and will be useful for understanding and developing biofilm-based processes.

Introduction

Clostridium perfringens is a Gram-positive anaerobic bacterium that causes numerous human and animal diseases [1]. A classification system based on the production of four major toxins (alpha, beta, epsilon, and iota) divides *C. perfringens* into five pathogenic types (A–E) [2]. *C. perfringens* type A is responsible for food poisoning and gas gangrene, and currently, *C. perfringens* type A food poisoning ranks as the second most commonly reported foodborne illness in Canada [3]. In addition, gas gangrene is considered one of the most menacing of human infections [4].

To persist in the environment, *C. perfringens* has evolved the ability to form biofilms, which provide some of the same protections afforded by endospores, but can more quickly respond to changes in the environment [5]. Biofilms, the predominant state of bacteria in nature [6], are structured communities of bacterial cells enclosed in a self-produced extracellular polysaccharide matrix [7]. The type IV pilus and the catabolite control protein CcpA are essential for maximum biofilm formation by *C. perfringens* [5]. In addition, the *C. perfringens* Agr-like system regulates biofilm formation by increasing the levels of the *C. perfringens* alpha-toxin and the perfringolysin O toxin [8]. A sporulation factor is also involved in the morphological changes of *C. perfringens* biofilms in response to temperature [9].

Biofilm formation is involved bacterial pathogenesis [10], with biofilm formation shown to be a major factor in the pathogenesis of *Pseudomonas aeruginosa* lung infections [11] and *Staphylococcus epidermidis* infections involving medical implants [12]. Biofilm formation by *C. perfringens* causes antibiotic-associated diarrhoea [13], even with suitable antibiotic treatment [9]. This is because the biofilm

✉ Guisheng Ye
   qhxjygs@163.com

1 State Key Laboratory of Plateau Ecology and Agriculture, Qinghai University, Xining, Qinghai 810016, China

2 College of Agriculture and Animal Husbandry, Qinghai University, No 251. Ningda Road, Chengbei District, Xining, Qinghai 810016, China

protects the cells from exposure to atmospheric oxygen and to high concentrations of antibiotics [14].

Very little is known about the differences in gene expression between biofilm-associated and planktonic *C. perfringens* cells. Charlebois et al. showed that 772 genes were significantly differentially expressed between biofilms and planktonic cells collected from the supernatant of biofilms [15]. Although genetic studies of *C. perfringens* biofilms have been conducted, differentially expressed genes (DEGs) have not yet been described in detail. Therefore, this study was undertaken to investigate the morphology and gene expression of *C. perfringens* biofilms. The findings described here should be highly useful for understanding and developing biofilm-based processes using *C. perfringens*.

Materials and Methods

Bacterial Growth Conditions and Biofilm Formation

C. perfringens Type A strain CICC 22949 was purchased from the China Center of Industrial Culture Collection. Bacteria were cultured at 37 °C for 24 h in fluid thioglycollate (FT) medium (Beijing Land Bridge Technology Co., Beijing, China) sealed with paraffin. Biofilms were cultured as described previously [14], with some modifications. Briefly, overnight FT cultures of *C. perfringens* were washed in FT supplemented with 10 mM (final concentration) filter-sterilized glucose (Beijing Solarbio Science & Technology Co., Beijing, China) and resuspended to an OD_{600} of 0.08–0.1. Aliquots (10 ml) of the cell suspension were then added to 100 mm × 20 mm dishes (Corning Incorporated, One Riverfront Plaza, Corning, NY 14831, USA) and incubated anaerobically at 37 °C for 3 days in an anaerobic jar containing anaeropacks (Mitsubishi Gas Chemical Co., Tokyo, Japan). Following incubation, medium containing planktonic cells was harvested; dishes were washed twice with sterilized physiological saline, and attached cells (biofilm) were removed using a cell scraper (Corning Incorporated, One Riverfront Plaza, Corning, NY 14831, USA). The harvested cells were then resuspended in 1 ml of sterilized normal saline for use in further experiments. Samples were examined in triplicate and the experiment was repeated three times.

Visualization of Biofilms

SEM was performed to visualize the surfaces of *C. perfringens* biofilms. Biofilms were then cultured as described above and incubated for 12, 24, 48, or 72 h. The dishes were washed twice with sterilized normal saline to remove unattached cells, then immersed in 2.5% glutaraldehyde overnight to fix the cells. Subsequently, the dishes were rinsed twice in sterilized normal saline and dehydrated sequentially in 30, 50, 70, 90, and 99.5% ethanol. To allow observation of the biofilms under the SEM, the dishes containing the biofilms were cut into 1 cm²-sections, then sputter-coated under vacuum with a 5-nm-thick layer of gold using a SBC-2 sputter coater (KYKY Technology Co., Beijing, China). Finally, the 1 cm²-sections were observed using a JSM-6610LV scanning electron microscope (JEOL Ltd., Japan).

Transcriptomic Analysis

RNA Extraction, Library Construction, and RNA Sequencing

Total RNA from planktonic and biofilm-associated cells was extracted using an EASY Spin Plus Tissue/Cell RNA Extraction Kit (Beijing Aidlab Biotechnologies Co., Beijing, China) as described by the manufacturer. RNA integrity and purity were verified using a NanoPhotometer spectrophotometer (IMPLEN, CA, USA) and a RNA Nano 6000 Assay Kit of the Bioanalyzer 2100 system (Agilent Technologies, CA, USA), respectively. cDNA libraries were constructed using a NEBNext® Ultra™ RNA Library Prep Kit for Illumina® and sequenced using an Illumina HiSeq-PE150 platform by Novogene Bioinformatics Technology Co. (Beijing, China).

Data Quality Assessment, Mapping, and Quantification of Gene Expression

The raw reads were cleaned by removing reads with adapters, reads in which unknown bases accounted for > 10% of the sequence length, and low-quality reads. Q20 and Q30 values (proportion of nucleotides with quality values larger than 20 and 30, respectively) were then calculated To quantify gene expression levels, clean reads were mapped to reference sequences using Bowtie 2 [16]. The levels of gene expression were calculated using the reads per kb transcriptome per million mapped reads method for each sample.

Screening of DEGs

Differential expression analysis of the two samples was conducted using the DEGseq package [17]. *P* values were adjusted using the *q* value, where a *q* value < 0.005 was set as the threshold for significant differential expression. If the $\log_2$(fold change) value was > 0, the expression of the DEG was determined to be up-regulated, whereas if the $\log_2$(fold change) value was < 0, the DEG was down-regulated.

GO and KEGG Pathway Enrichment Analysis of DEGs

GO enrichment analysis of the DEGs was implemented in the GOseq package [18]. GO terms for which the corrected

P value was < 0.05 were defined as significantly enriched. KEGG pathway analysis of the DEGs was then conducted using KOBAS, and pathways with a corrected *P* value of ≤ 0.05 were considered to be significantly enriched amongst the DEGs.

qRT-PCR Analysis

RNA was converted to first-strand cDNA using a Prime-Script RT Reagent Kit with gDNA Eraser (Perfect Real Time) (TaKaRa, Dalian, China) as per the manufacturer's instructions. Five DEGs (CPF_RS01050, CPF_RS11985, CPF_RS13235, CPF_RS13265, CPF_RS01780) were randomly chosen for validation by qRT-PCR analysis. GAPDH was selected as an internal control. Primers were designed and manufactured by Takara Biosciences (Dalian, China). Primer sequences are listed in Table 1. Three replicates were prepared for each gene in each qRT-PCR assay. The reaction mixtures (25 µl) consisted of 12.5 µl of SYBR Premix DimerEraser (2×), 0.75 µl (10 µM) of each of the forward and reverse primers, 2 µl of cDNA (35 ng), and 9 µl of ddH$_2$O. Thermal cycler parameters consisted of an initial denaturation at 95 °C for 30 s, followed by 40 cycles of 95 °C for 5 s, 55 °C for 30 s, and 72 °C for 30 s, followed by melting curve analysis from 65 to 95 °C using a CFX96 Real Time System (BioRad, USA). The relative levels of each of the amplified mRNAs were evaluated according to the $2^{-\triangle\triangle Ct}$ method.

Table 1 Primers used for q RT-PCR analysis

Gene name	Sequence (5′–3′)	Product length (bp)
GAPDH	F: ATTCTGGGATAACTAAACCGA TAGC R: CACGCTTACACTAACGACCAA AAC	139
CPF_RS01050	F: AATAGGCGAAACTGCTCCTGAA R: CATACCATAGATTGTTCTTCC ACCA	91
CPF_RS11985	F: TTTCCCAGTATCTCTTGCACTACG R: GGCATACCTAATTGAGCAAACCA	117
CPF_RS13235	F: GTGGTAGAAACGCACAAGGTA AAA R: CTTCTCTCCATCAGCATAAAC AACA	182
CPF_RS13265	F: GAAACCACAAAATAGGGGAAA CTC R: GCCGTACTTGTCTGCCTGTCT	275
CPF_RS01780	F: AATGGAAGACGTTCCTTCAGTTC R: CTCTTGTTGGTCTTGGGTTTCTC	122

Results

Visualization of *C. perfringens* Biofilms

C. perfringens strain CICC 22949 was tested for biofilm formation following incubation on plastic surfaces. Evidence of biofilm formation was examined using SEM, which showed that as the incubation time progressed, the number of bacteria attached to the surface increased gradually. SEM images showed the cells encased in a dense, self-secreted matrix material, which gradually formed into a biofilm of aggregated masses (Fig. 1).

Transcriptomic Analysis

Differential Expression Analysis

Quality assessment results for the sequencing data are shown in Table 2, and confirmed that the Illumina sequencing was of high quality. RNA sequencing analysis identified 91 genes that were significantly differentially expressed in the two growth modes (Fig. 2). Of these, 40 were up-regulated and 51 were down-regulated in biofilms. In particular, genes encoding sortase, ribosomal proteins, and ATP synthase were up-regulated in biofilms, while genes coding for clostripain and phospholipase C were down-regulated.

GO Enrichment Analysis

To better understand the functional differences in gene expression, the biological functions of the DEGs were characterized by GO enrichment analysis. We divided the enriched terms into up-regulated and down-regulated groups (Fig. 3). The up-regulated DEGs were divided into 32 significantly enriched GO terms, including 24 in biological process, four in molecular function, and four in cellular component. The up-regulated DEGs were most commonly associated with the "macromolecular complex" category. The gene (CPF_RS03835) encoding sortase was enriched in 19 GO pathways related to membrane, catalytic activity, quorum sensing, pathogenesis, and so on. Interestingly, no GO terms were significantly enriched for the down-regulated DEGs.

KEGG Pathway Enrichment Analysis

We also conducted KEGG pathway enrichment analysis of the DEGs to further characterize their biological functions. A scatter diagram was generated showing the degree of KEGG enrichment, which was measured by means of rich factor, *q* value, and the number of genes enriched for a
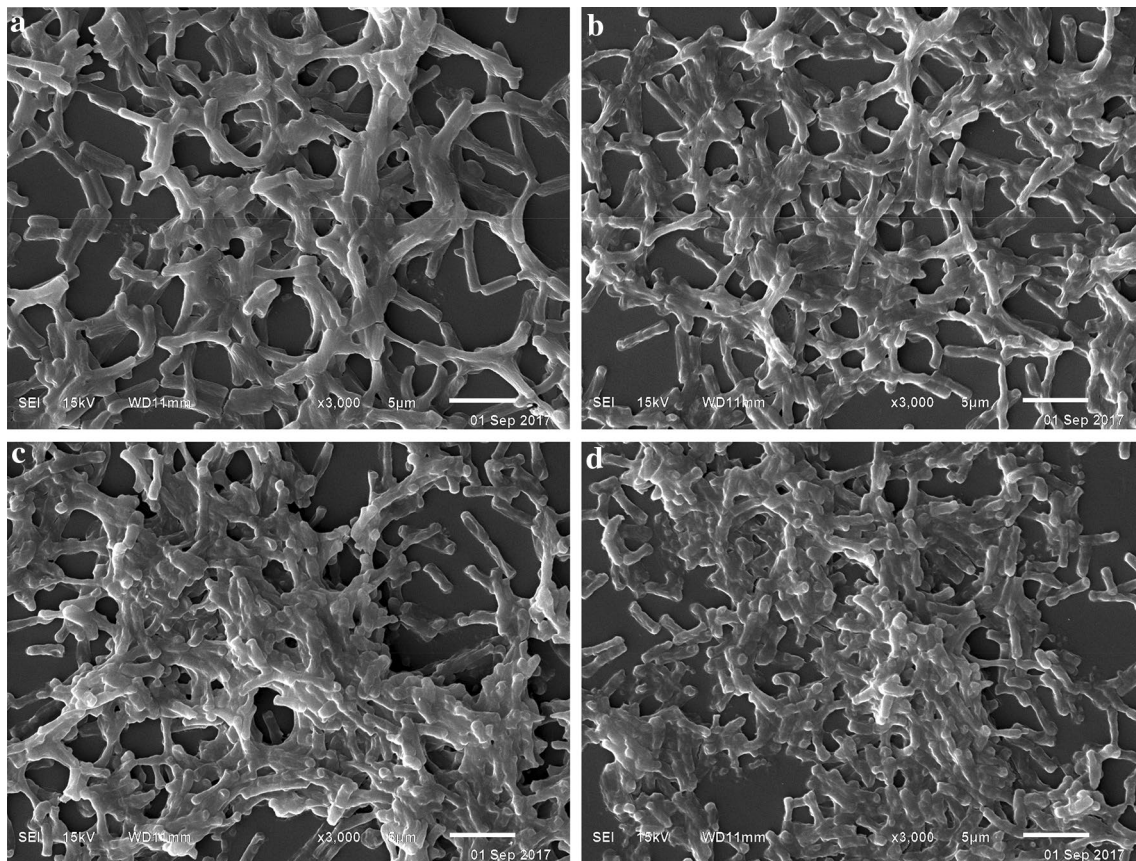
Fig. 1 Morphological observation of *C. perfringens* biofilm by SEM. Biofilms were cultured for 12 h (**a**), 24 h (**b**), 48 h (**c**), or 72 h (**d**)

Table 2 Quality assessment of sample sequencing data

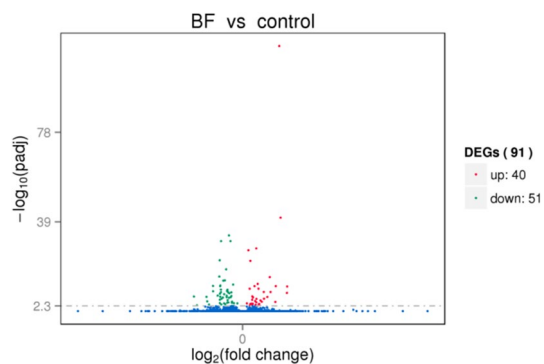| Sample name	Raw reads	Clean reads	Clean bases	Error rate (%)	Q20 (%)	Q30 (%)
Control	19040344	18734016	2.81G	0.02	97.31	92.93
BF	17797076	17509536	2.63G	0.02	97.32	92.96

Fig. 2 Volcano figure of differentially expressed genes. Scattered dots represent individual genes, where blue dots indicate the unigenes with no significant differential expression; red dots indicate the significantly up-regulated unigenes, and green dots indicate the significantly down-regulated unigenes

particular pathway. Of the 33 KEGG pathways associated with the DEGs, the 20 most enriched pathway are shown in Fig. 4. Among the 20 pathways, oxidative phosphorylation was the only significantly enriched pathway (Fig. 5), and included genes encoding the ATP synthase subunit alpha, the ATP synthase subunit beta, the F_0F_1 ATP synthase subunit A, the ATP synthase subunit b, and cobalt-dependent inorganic pyrophosphatase.

qRT-PCR Validation of RNA Sequencing

To validate the RNA sequencing results, qRT-PCR analysis was performed using five randomly selected DEGs, which encoded heme oxygenase (CPF_RS01050), F0F1 ATP synthase subunit A (CPF_RS11985), 50S ribosomal protein L2 (CPF_RS13235), elongation factor G (CPF_RS13265)
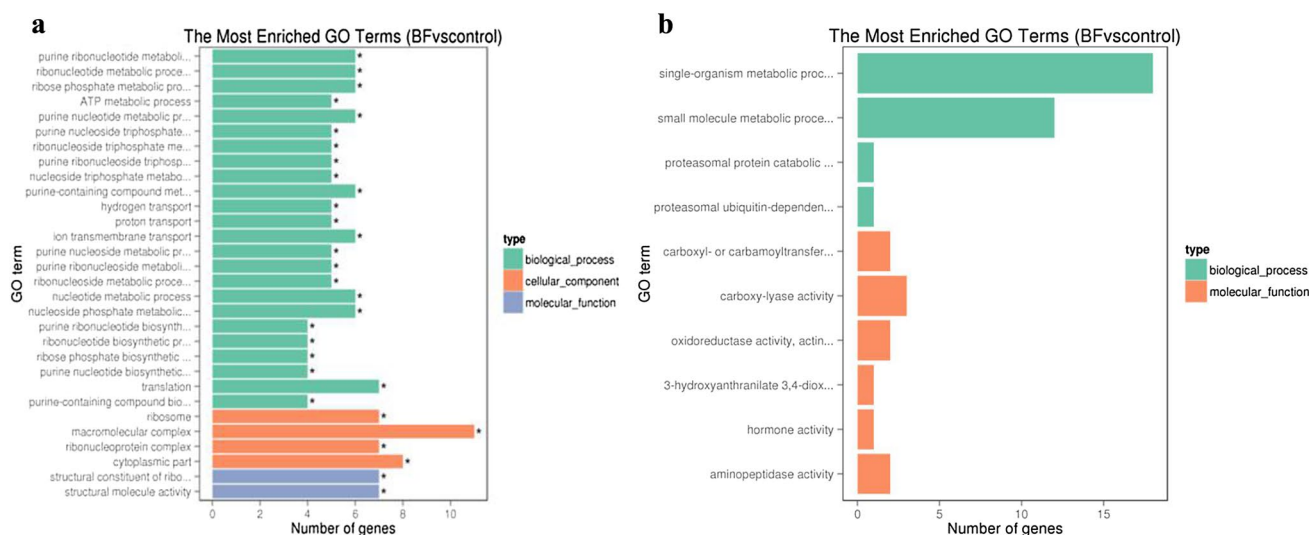
Fig. 3 Gene ontology classifications of unigenes. **a** Enriched GO terms of up-regulated DEGs. **b** Enriched GO terms of down-regulated DEGs
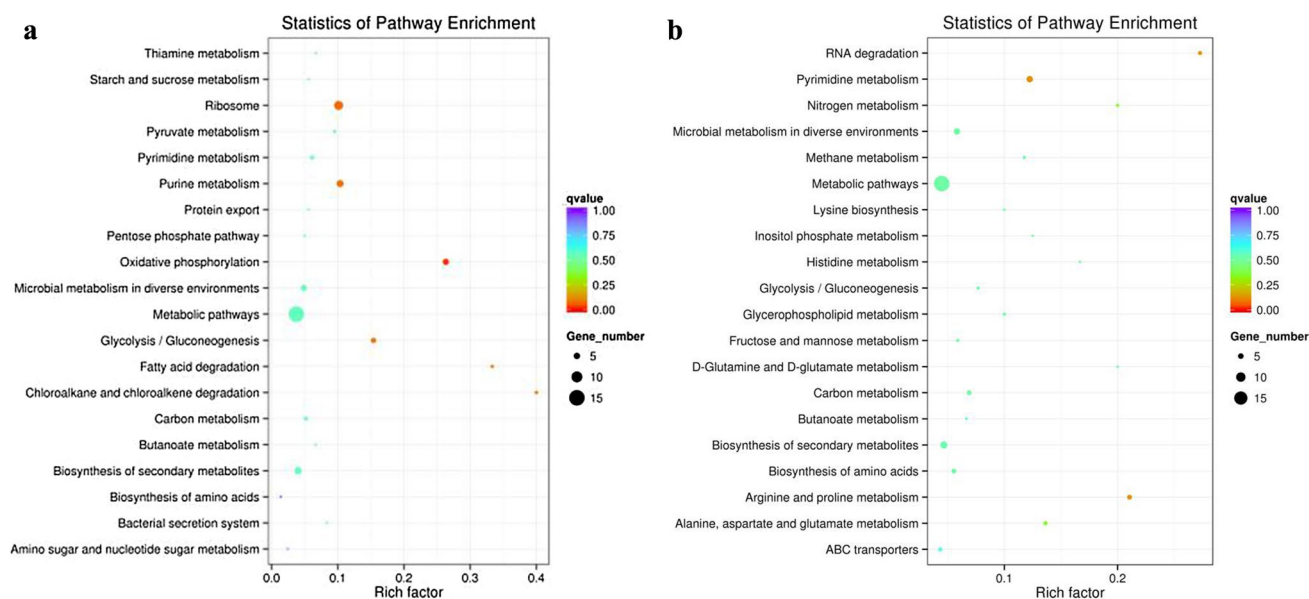

Fig. 4 Scatter diagram of pathway enrichment. The size of the dot indicates the number of differentially expressed genes (DEGs) in the pathway, and the point colours correspond to different *q* value ranges, with numbers closer to zero indicating more significant enrichment, *q* value of <0.05 was considered to be significantly enriched. Rich factor refers to the ratio of the number of DEGs versus the number of annotated genes in a pathway. The greater the rich factor, the greater the degree of enrichment. **a** Pathways with up-regulated DEGs. **b** Pathways with down-regulated DEGs

and pyruvate kinase (CPF_RS01780). The gene expression ratios were calculated after the expression levels of each gene were normalized against those of the constitutively expressed gene, *GAPDH*. The result showed that all five genes were up-regulated (Fig. 6), which was in accordance with the results of RNA sequencing.

Discussion

This study showed that genes encoding clostripain and phospholipase C were down-regulated in biofilms. This result is in agreement with previous findings that toxin
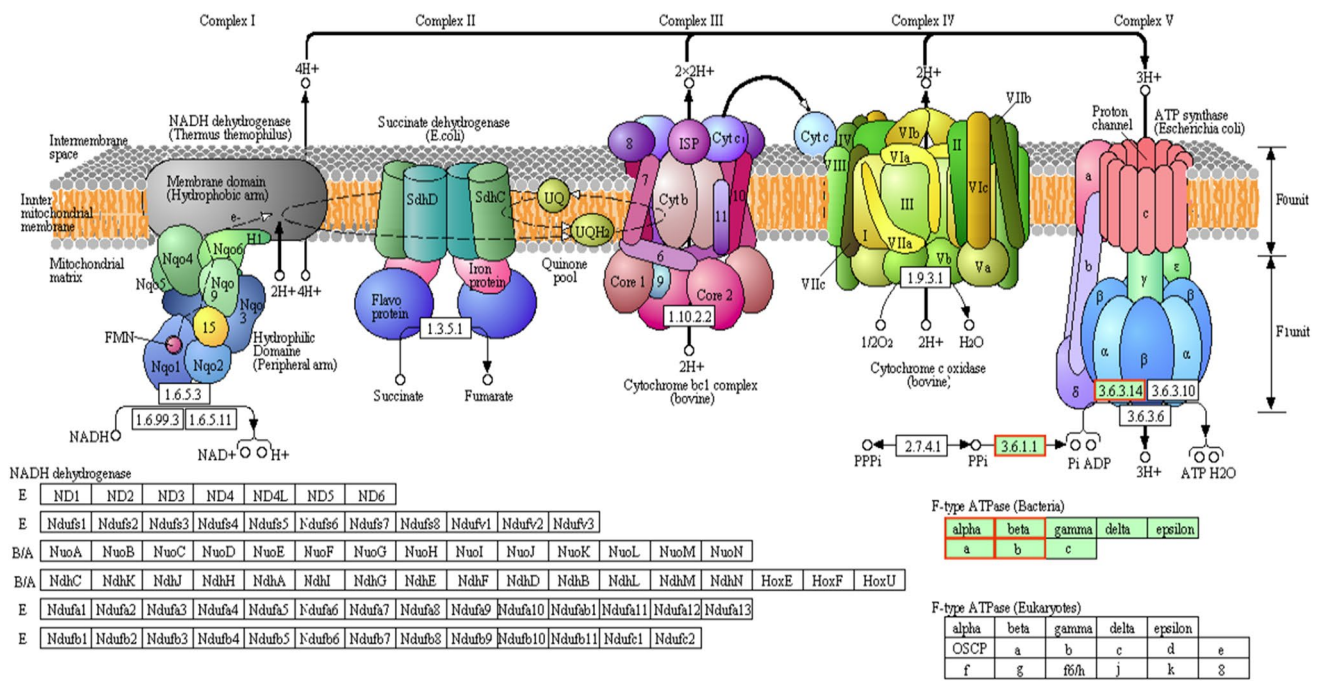
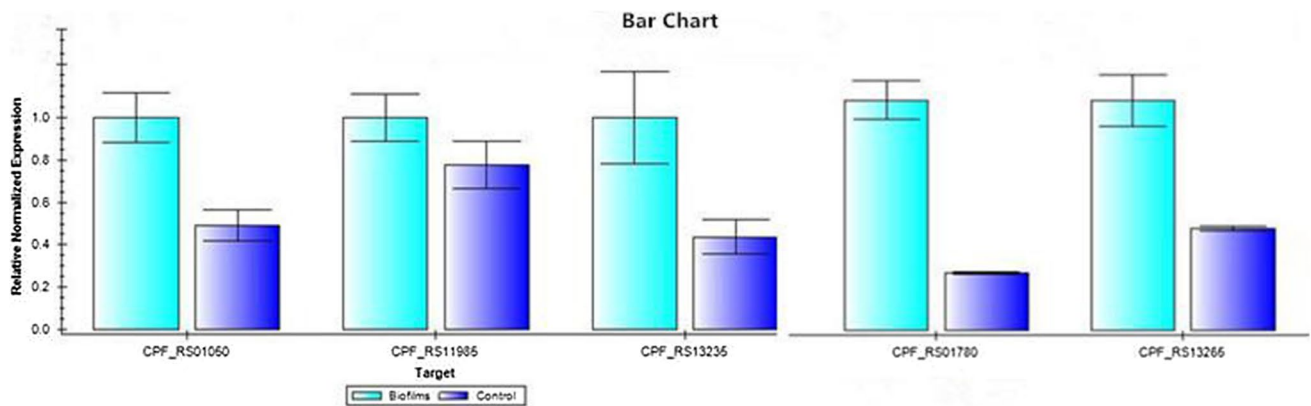**Fig. 5** Oxidative phosphorylation pathway

Fig. 6 Relative expression levels of DEGs

genes are down-regulated in *C. perfringens* biofilms [15], suggesting that toxin genes do not contribute to the persistence of the *C. perfringens* biofilm. However, another study showed that the toxin regulator CtrAB is required for *C. perfringens* pellicle biofilm formation at 25 °C as it is involved in extracellular matrix production, and thereby regulates the morphological changes of the biofilm in response to temperature. Nevertheless, CtrAB was not needed for adhered-biofilm formation at 37 °C [9]. In addition, *plc*, encoding alpha-toxin phospholipase C, was more active at 25 °C than at 37 °C in biofilms [9]. These findings imply that temperature affects the expression of *C. perfringens* toxin genes in a biofilm. At

optimum growth temperatures, the expression of toxin genes is likely reduced during *C. perfringens* biofilm formation, whereas at lower temperatures, toxin genes may be involved in extracellular matrix production to increase the resistance of the bacterium to the changed environment. However, the mechanisms underlying toxin gene expression in *C. perfringens* biofilms have not yet been clearly demonstrated, and further investigation is needed.

In the present study, many genes involved in the macromolecular complex were up-regulated in biofilm-associated cells, including 50S ribosomal protein L2, L4, L7/L12, L17, L20, L27, S20, and a VWA domain-containing protein. A temperature-sensitive mutation in *rplB*, encoding ribosomal

protein L2, caused growth and sporulation defects in *Bacillus subtilis* [19], while a sporulation factor was involved in the morphological changes of *C. perfringens* biofilms in response to temperature [9]. Thus, we hypothesize that biofilm formation is closely associated with ribosomal protein L2, which is essential for both growth and sporulation. L27 was suggested to contribute to the function of the ribosomal peptidyl transferase centre via interactions between its *N*-terminal tail and both the A- and P-site tRNAs [20]. These 50S ribosomal proteins may be used to interact with translation factors, which is essential for protein synthesis.

This study showed that the gene encoding sortase was up-regulated in biofilms, and enriched in the GO pathways related to membrane, catalytic activity, quorum sensing, pathogenesis and so on. Sortase catalyses the attachment of surface proteins and pili to the peptidoglycan layer of Gram-positive bacteria [21]. Sortases can be divided into four subfamilies, SrtA–D. *C. perfringens* has both a SrtA and a SrtC. SrtA is responsible for sorting and anchoring surface proteins to the cell wall, while SrtC catalyses the head-to-tail assembly of the pilins into the final polymerized form. Numerous genetic knockout experiments have shown that SrtA plays a critical role in the pathogenesis of Gram-positive bacteria by modulating the ability of the bacterium to adhere to host tissue [22]. In addition, sortase-dependent pili play an important role in the development of pathogenic biofilm communities. For example, the adhesive pilus found in *Streptococcus* and *Actinomyces* strains contributes to the early stages of biofilm growth by participating in the primary attachment of bacterial cells to saliva-coated tooth surfaces, which eventually results in dental plaques and caries [23–25]. Further, pilus-driven accumulation of bacteria into a biofilm often hinders or delays wound healing [26]. In *C. perfringens* biofilms, type IV pilus-dependent gliding motility is necessary for efficient biofilm formation, and is not associated with the bacteria in the biofilm, but with the extracellular matrix [5]. Therefore, these findings indicate that sortase is an essential virulence factor for *C. perfringens* biofilm formation. Based on this theory, sortase may be a promising target for new anti-infective drugs, which are desperately needed due to the current lack of antibiotic therapy options for drug-resistant *C. perfringens* strains.

KEGG analysis showed that genes involved in oxidative phosphorylation were up-regulated in biofilms. In *Shewanella oneidensis*, metabolic energy is directly or indirectly required to maintain the stability of microbial biofilms. A previous study showed that in *S. oneidensis* MR-1 biofilms at 12-h post-inoculation, a reduction in cellular ATP concentration, induced by addition of the inhibitor of carbonyl cyanide m-chlorophenylhydrazone, resulted in a massive dissolution of the biofilm structure [27]. These findings suggest that ATP is required for biofilm stability, which is in line with our findings that the genes encoding ATP synthase and cobalt-dependent inorganic pyrophosphatase are particularly important in *C. perfringens* biofilm formation.

In this study, the glycolysis/gluconeogenesis pathway was enriched in the biofilm cells. In *Streptococcus gordonii*, carbohydrates induced biofilm formation [28], and in *B. subtilis*, some glucose was required for biofilm formation [29]. Likewise, 10 mM glucose is needed for maximal *C. perfringens* biofilm formation. While strains suppress biofilm formation in favour of planktonic growth as the concentration of glucose in the medium increases (25–100 mM), the highest ratio of biofilm to planktonic cells was observed in the absence of glucose [5]. This suggests that biofilm formation is induced in the absence of carbohydrates to enhance bacterial survival. Therefore, the glycolysis/gluconeogenesis pathway likely regulates biofilm formation under different glucose concentrations.

In summary, this study provides information on the morphology of *C. perfringens* biofilms after 12, 24, 48, and 72 h of incubation. The cells could be seen encased in a dense, self-secreted matrix material, and the biomass of the biofilm increased gradually with incubation time. This study also revealed *C. perfringens* genes that are differentially expressed during biofilm formation. Genes coding for sortase, ATP synthase, and ribosomal structure proteins were up-regulated, whereas genes coding for clostripain and phospholipase C was down-regulated in biofilm cells. Moreover, as oxidative phosphorylation was a significantly enriched pathway, we suggest that metabolic energy may be required for the stability of *C. perfringens* biofilms. Besides, the glycolysis/gluconeogenesis pathway was enriched in the biofilm cells, it likely regulates biofilm formation under different glucose concentrations.

Compliance with Ethical Standards

Conflict of interest The authors declare that they have no conflict of interest.

References

1. Charlebois A, Jacques M, Boulianne M, Archambault M (2017) Tolerance of *Clostridium perfringens* biofilms to disinfectants commonly used in the food industry. Food Microbiol 62:32–38
2. Petit L, Gibert M, Popoff MR (1999) *Clostridium perfringens*: toxinotype and genotype. Trends Microbiol 7(3):104–110
3. Thomas MK, Murray R, Flockhart L, Pintar K, Pollari F, Fazil A, Nesbitt A, Marshall B (2013) Estimates of the burden of foodborne illness in Canada for 30 specified pathogens and unspecified agents, circa 2006. Foodborne Pathog Dis 10(7):639–648
4. Bryant AE (2003) Biology and pathogenesis of thrombosis and procoagulant activity in invasive infections caused by group A

streptococci and *Clostridium perfringens*. Clin Microbiol Rev 16(3):451–462

5. Varga JJ, Therit B, Melville SB (2008) Type IV pili and the CcpA protein are needed for maximal biofilm formation by the gram-positive anaerobic pathogen *Clostridium perfringens*. Infect Immun 76(11):4944–4951

6. Davey ME, O'Toole GA (2000) Microbial biofilms: from ecology to molecular genetics. Microbiol Mol Biol Rev 64(4):847–867

7. Costerton JW, Stewart PS, Greenberg EP (1999) Bacterial biofilms: a common cause of persistent infections. Science 284(5418):1318–1322

8. Jorge EV, Joshua RS, Canizalez-Roman A (2015) The CpAL quorum sensing system regulates production of hemolysins CPA and PFO to build *Clostridium perfringens* biofilms. Infect Immun 83(6):2430–2442

9. Obana N, Nakamura K, Nomura N (2014) A Sporulation factor is involved in the morphological change of *Clostridium perfringens* biofilms in response to temperature. J Bacteriol 196(8):1540–1550

10. Høiby N, Bjarnsholt T, Givskov M, Molin S, Ciofu O (2010) Antibiotic resistance of bacterial biofilms. Int J Antimicrobial Agents 35(4):322–332

11. Costerton JW (2001) Cystic fibrosis pathogenesis and the role of biofilms in persistent infection. Trends Microbiol 9(2):50–52

12. Ha KY, Chung YG, Ryoo SJ (2005) Adherence and biofilm formation of *Staphylococcus epidermidis* and *Mycobacterium tuberculosis* on various spinal implants. Spine 30(1):38–43

13. Modi N, Wilcox MH (2001) Evidence for antibiotic induced *Clostridium perfringens* diarrhoea. J Clin Pathol 54(10):748–751

14. Charlebois A, Jacques M, Archambault M (2014) Biofilm formation of *Clostridium perfringens* and its exposure to low-dose antimicrobials. Front Microbiol 5:183

15. Charlebois A, Jacques M, Archambault M (2016) Comparative transcriptomic analysis of *Clostridium perfringens* biofilms and planktonic cells. Avian Pathol 45(5):593–601

16. Langmead B, Salzberg SL (2012) Fast gapped-read alignment with Bowtie 2. Nat methods 9(4):357–359

17. Wang L, Feng Z, Wang X, Wang X, Zhang X (2010) DEGseq: an R package for identifying differentially expressed genes from RNA-seq data. Bioinformatics 26(1):136–138

18. Young MD, Wakefield MJ, Smyth GK, Oshlack A (2010) Gene ontology analysis for RNA-seq: accounting for selection bias. Genome Biol 11(2):R14

19. Suzuki S, Tanigawa O, Akanuma G, Nanamiya H, Kawamura F, Tagami K, Nomura N, Kawabata T, Sekine Y (2014) Enhanced expression of *Bacillus subtilis* yaaA can restore both the growth and the sporulation defects caused by mutation of rplB, encoding ribosomal protein L2. Microbiology 160(Pt 6):1040–1053

20. Maracci C, Wohlgemuth I, Rodnina MV (2015) Activities of the peptidyl transferase center of ribosomes lacking protein L27. RNA 21(12):2047–2052

21. Schmohl L, Bierlmeier J, von Kügelgen N, Kurz L, Reis P, Barthels F, Mach P, Schutkowski M, Freund C, Schwarzer D (2017) Identification of sortase substrates by specificity profiling. Bioorg Med Chem 25(18):5002–5007

22. Jonsson IM, Mazmanian SK, Schneewind O, Bremell T, Tarkowski A (2003) The role of *Staphylococus aureus* sortase A and sortase B in murine arthritis. Microbes Infect 5(9):775–780

23. Mishra A, Devarajan B, Reardon ME, Dwivedi P, Krishnan V, Cisar JO, Das A, Narayana SV, Ton-That H (2011) Two autonomous structural modules in the fimbrial shaft adhesin FimA mediate Actinomyces interactions with streptococci and host cells during oral biofilm development. Mol Microbiol 81(5):1205–1220

24. Mishra A, Wu C, Yang J, Cisar JO, Das A, Ton-That H (2010) The Actinomyces oris type 2 fimbrial shaft FimA mediates co-aggregation with oral streptococci, adherence to red blood cells and biofilm development. Mol Microbiol 77(4):841–854

25. Okahashi N, Nakata M, Terao Y, Isoda R, Sakurai A, Sumitomo T, Yamaguchi M, Kimura RK, Oiki E, Kawabata S, Ooshima T (2011) Pili of oral Streptococcus sanguinis bind to salivary amylase and promote the biofilm formation. Microb Pathog 50(3–4):148–154

26. Metcalf DG, Bowler PG (2013) Biofilm delays wound healing: a review of the evidence. Burns Trauma 1(1):5–12

27. Saville RM, Rakshe S, Haagensen JA, Shukla S, Spormann AM (2011) Energy-dependent stability of *Shewanella oneidensis* MR-1 biofilms. J Bacteriol 193(13):3257–3264

28. Gilmore KS, Srinivas P, Akins DR, Hatter KL, Gilmore MS (2003) Growth, development, and gene expression in a persistent *Streptococcus gordonii* biofilm. Infect Immun 71(8):4759–4766

29. Stanley NR, Britton RA, Grossman AD, Lazazzera BA (2003) Identification of catabolite repression as a physiological regulator of biofilm formation by *Bacillus subtilis* by use of DNA microarrays. J Bacteriol 185(6):1951–1957